# Systematic optimization of long-range corrected hybrid density functionals

Jeng-Da Chai[a)] and Martin Head-Gordon[b)]

*Department of Chemistry, University of California and Chemical Sciences Division, Lawrence Berkeley National Laboratory, Berkeley, California 94720, USA*

A general scheme for systematically modeling long-range corrected (LC) hybrid density functionals is proposed. Our resulting two LC hybrid functionals are shown to be accurate in thermochemistry, kinetics, and noncovalent interactions, when compared with common hybrid density functionals. The qualitative failures of the commonly used hybrid density functionals in some "difficult problems," such as dissociation of symmetric radical cations and long-range charge-transfer excitations, are significantly reduced by the present LC hybrid density functionals. © *2008 American Institute of Physics.* [DOI: 10.1063/1.2834918]

## I. INTRODUCTION

In the last two decades, density functional theory[1] (DFT) based on the Kohn–Sham (KS) approach[2,3] has been attracting considerable attention.[4,5] Due to its favorable scaling with system size and reasonable accuracy in many applications, KS-DFT has been regarded as one of the most powerful theoretical tools for studying both electronic and dynamic properties of medium to large ground-state systems. Recently, the development of time-dependent density functional theory (TDDFT) for treating excited-state systems has also been making considerable progress.[6,7]

In KS-DFT, the exact exchange-correlation energy functional $E_{xc}[\rho]$, however, remains unknown, and needs to be approximated. Functionals based on the local spin density approximation (LSDA) have been successful for nearly-free-electron systems.[4,5] However, for molecular systems, where electron densities are highly nonuniform, the severe overbinding tendency of LSDA means it is not sufficiently accurate for most quantum chemical applications.

Functionals based on the semilocal generalized gradient approximations (GGAs) have considerably reduced the errors associated with the LSDA and have shown reasonable accuracy for atomization energies of many strongly bound systems.[8] For some weakly bound systems, such as hydrogen-bonded systems, GGAs are still reasonable for the energetics and geometries. However, GGAs can completely fail for van der Waals systems. For such systems, GGAs give insufficient binding or even unbound results. Moreover, GGAs tend to give predicted barrier heights of chemical reactions that are usually seriously underestimated.

Both of the LSDA and GGAs (commonly denoted as DFAs for density functional approximations) are based on the localized model exchange-correlation holes. The exact exchange-correlation hole is, however, fully nonlocal. Therefore, the success of DFAs is commonly believed to be due to a cancelation of errors between the DFAs for exchange and correlation.[4,5] In situations where the cancelation of errors is not complete, the DFAs can produce erroneous results. Noticeably, some of these situations occur in the asymptotic regions of molecular systems, where the electron densities decay exponentially. In such regions, due to the severe self-interaction error (SIEs) of DFAs, the DFA exchange-correlation potential exhibits an exponential decay, instead of the correct $-1/r$ decay. This leads to many qualitative failures for problems such as dissociation of cations with odd number of electrons or even the alkali halides.[9,10] In time-dependent DFT, SIE causes dramatic failures for long-range charge-transfer excitations of two well-separated molecules.[11–13] The spatially localized nature of DFAs also leads to the absence of London forces, which are a long-range correlation effect. Therefore, to circumvent the above difficulties, it seems necessary to incorporate part or all of the nonlocality of the exchange-correlation hole into the DFAs.

Hybrid DFT methods, which combine KS-DFT with wave function theory (WFT), are promising as a cost-effective way to incorporate nonlocality of the exchange-correlation hole into the DFAs. They can provide reasonable accuracy for treating large-scale systems. In fact, the most widely used density functionals in quantum chemistry are all hybrid functionals! This happy marriage of KS-DFT and WFT was first proposed by Becke,[14] who argued that mixing a small fraction of the exact Hartree–Fock (HF) exchange (associated with the Kohn–Sham reference wave function) with DFAs will provide the desired nonlocality and thereby generally improve the DFA results. The general form of a hybrid density functional can be written as

$$E_{xc} = c_x E_x^{HF} + E_{xc}^{DFA}, \tag{1}$$

where $c_x$ is a small fractional number, typically ranging from 0.2 to 0.25 for thermochemistry,[14] and from 0.4 to 0.6 for kinetics.[15]

Indeed, a remarkable accuracy has been achieved by hybrid density functionals. For example, one of the most widely used hybrid density functionals, B3LYP,[14,16] a combination of the B88 exchange functional[17] and the LYP correlation functional,[18] has achieved a better accuracy for

---

a)Electronic mail: jdchai@berkeley.edu.
b)Author to whom correspondence should be addressed. Electronic mail: mhg@cchem.berkeley.edu.

many strongly bound systems than the second-order Moller-Plesset perturbation theory (MP2).[19] Since then, there have been considerable efforts to improve $E_{xc}[\rho]$ relative to B3LYP. The development of hybrid density functionals has facilitated the transition of KS-DFT from solid-state physics into the realm of quantum chemistry as well.

In 1997, another significant advance in KS-DFT was also made by Becke, who proposed to model exchange-correlation functionals by a systematic procedure.[20] Similar to expanding molecular orbitals by linear combinations of atomic orbitals, he proposed to expand $E_{xc}[\rho]$ using power series expansions involving only the local spin density and its first derivative, in addition to a small fraction of the HF exchange. The linear coefficients in the expansions are optimized from a systematic fitting procedure to a set of reliable experimental data (the so-called training set). Due to the high flexibility of his functional forms, his resulting B97 functional has achieved impressive accuracy for thermochemistry. Since then, additional attempts have been made to devise good *basis functionals*, which have led to many quite accurate $E_{xc}[\rho]$, such as VSXC,[21] B97-1,[22] B97-2,[23] B97-3,[24] BMK,[15] the HCTH family,[22,25,26] and M05-2X.[27]

However, a few serious problems still remain in these *global* hybrid density functionals. As can been seen from Eq. (1), the exchange-correlation potential decays as $-c_X/r$, not the correct $-1/r$ decay. This still leads to qualitatively incorrect results for charge-transfer (CT) excited states of molecules.[11–13] Although the use of full HF exchange may remedy these difficulties, a DFA for correlation is, however, incompatible with the fully nonlocal HF exchange due to the absence of good cancelation of errors between them, although efforts to develop entirely new post-Hartree–Fock correlation functionals show promise.[28] A similar difficulty applies to optimized effective potential approaches at present.[29]

To make progress, the long-range corrected (LC) hybrid density functionals have been receiving increasing attention.[30–44] LC hybrids retain full HF exchange only for long-range electron-electron interactions (i.e., the asymptotic regime), and thereby resolve a significant part of the self-interaction problems associated with global hybrid functionals. However, the currently used LC hybrid functionals are still not as accurate as the best global hybrid functionals, especially for thermochemistry.

Aiming to improve on this situation, here we propose suitable basis functionals for constructing LC hybrid density functionals. Our two resulting LC hybrid density functionals are shown to be accurate in many applications, such as thermochemistry, kinetics, and noncovalent interactions, when compared with the widely used global hybrid functionals. The rest of this paper is organized as follows. In Sec. II, we briefly describe the rationale for the LC hybrid approach. In Sec. III, we propose the suitable basis functionals for systematically generating accurate LC hybrid functionals. The performance of the two new LC hybrid functionals is compared with that of other functionals in Sec. IV (on the training set), and in Sec. V (on some test sets). In Sec. VI, we give our conclusions.

## II. RATIONALE FOR THE LC HYBRID SCHEME

For the LC hybrid scheme, one first defines long-range (LR) and short-range (SR) operators to partition the Coulomb operator. In the first LC scheme, proposed by Savin and co-workers, the LR part is treated by WFT [such as configuration interaction (CI)], and the SR part is treated by DFT.[30–36] Its advantage is to reduce the cost of CI calculation in a finite set of one-electron basis functions, as the LR operator is chosen to be nonsingular at electron-electron coalescence (and hence the basis does not have to represent the cusp). Since DFAs perform well for the short-range interaction, this type of approach has been gaining some attention. However, the need for high-level WFT for the LR interaction and the need to develop a generally accurate SR exchange-correlation functionals still hinder its progress.

Using the LSDA expression for the SR exchange from Refs. 31 and 45, a simplified LC hybrid scheme was first proposed by Iikura *et al.*[37] In this scheme, the LR exchange is treated exactly by HF theory, while the SR exchange is approximated by DFAs, and the correlation functional remains the same as that of the full Coulomb interaction,

$$E_{xc}^{LC-DFA} = E_x^{LR-HF} + E_x^{SR-DFA} + E_c^{DFA}. \qquad (2)$$

This greatly reduces the computational cost of the LC hybrid scheme, as the cost now is almost the same as the existing global hybrid scheme! In this work, we therefore focus on this type of LC hybrid scheme. The remaining problems are the choice of the SR and LR operators, the development of an accurate SR exchange density functional, and the development of a correlation functional that is compatible with it.

The most popular type of splitting operator used in the LC hybrid scheme is the standard error function (erf),

$$\frac{1}{r_{12}} = \frac{\text{erf}(\omega r_{12})}{r_{12}} + \frac{\text{erfc}(\omega r_{12})}{r_{12}}, \qquad (3)$$

where $r_{12} \equiv |\mathbf{r}_{12}| = |\mathbf{r}_1 - \mathbf{r}_2|$ (atomic units are used throughout this paper). On the right hand side of Eq. (3), the first term is long ranged, while the second term is short ranged. The parameter $\omega$ defines the range of these operators. In principle, different types of operators can also be used in the LC hybrid approaches. In this work, we employ the erf/erfc partition, as it is particularly straightforward to implement efficiently.[46]

For the simplest LC hybrid functional, the local spin density approximation is used for the DFAs. The LR HF exchange $E_x^{LR-HF}$ is computed by the occupied spin orbitals $\psi_{i\sigma}(\mathbf{r})$ with the LR operator,

$$\begin{aligned} E_x^{LR-HF} = -\frac{1}{2}\sum_\sigma \sum_{i,j}^{\text{occ.}} \int \int \psi_{i\sigma}^*(\mathbf{r}_1)\psi_{j\sigma}^*(\mathbf{r}_1) \\ \times \frac{\text{erf}(\omega r_{12})}{r_{12}}\psi_{i\sigma}(\mathbf{r}_2)\psi_{j\sigma}(\mathbf{r}_2)d\mathbf{r}_1 d\mathbf{r}_2, \end{aligned} \qquad (4)$$

while the analytical form of the SR LSDA exchange functional $E_x^{SR-LSDA}$ can be obtained by the integration of the square of the LSDA density matrix with the SR operator,[45]

$$E_x^{\text{SR-LSDA}} = \sum_\sigma \int e_{x\sigma}^{\text{SR-LSDA}}(\rho_\sigma) d\mathbf{r}. \tag{5}$$

Here, $e_{x\sigma}^{\text{SR-LSDA}}(\rho_\sigma)$ is the SR LSDA exchange energy density for $\sigma$-spin,

$$e_{x\sigma}^{\text{SR-LSDA}}(\rho_\sigma) = -\frac{3}{2}\left(\frac{3}{4\pi}\right)^{1/3} \rho_\sigma^{4/3}(\mathbf{r}) F(a_\sigma), \tag{6}$$

where $k_{F\sigma} \equiv (6\pi^2 \rho_\sigma(\mathbf{r}))^{1/3}$ is the local Fermi wave vector, and $a_\sigma \equiv \omega/(2k_{F\sigma})$ is a dimensionless parameter controlling the values of the attenuation function $F(a_\sigma)$,

$$F(a_\sigma) = 1 - \frac{8}{3}a_\sigma \left[ \sqrt{\pi}\, \text{erf}\left(\frac{1}{2a_\sigma}\right) - 3a_\sigma + 4a_\sigma^3 \right.$$
$$\left. + (2a_\sigma - 4a_\sigma^3)\exp\left(-\frac{1}{4a_\sigma^2}\right) \right]. \tag{7}$$

Retaining the LSDA correlation functional $E_c^{\text{LSDA}}$, one then has the simplest range-separated extended LDA (RSHX-LDA) hybrid functional,[39]

$$E_{\text{xc}}^{\text{RSHXLDA}} = E_x^{\text{LR-HF}} + E_x^{\text{SR-LSDA}} + E_c^{\text{LSDA}}. \tag{8}$$

The optimal $\omega$ values for RSHXLDA were found to be 0.5 bohr$^{-1}$ (Refs. 39) for molecular systems, and 0.4 bohr$^{-1}$ for solid-state systems.[40] However, due to its insufficient accuracy for thermochemistry, the development of gradient-corrected LC hybrid functionals continues attracting much attention, and will be our focus.

A relatively narrow range of $\omega$ values (from 0.2 to 0.5 bohr$^{-1}$). (Refs. 31, 32, 34, and 37–44) have been found for existing LC hybrid functionals by optimization of properties of interest. As can been seen in Eq. (3), the smaller the $\omega$ value is, the longer ranged the SR operator will be. As a result, the use of a small $\omega$ value in a LC hybrid functional implies that its SR exchange, which is actually not so short ranged, is approximated by spatially localized DFAs. Since the DFA exchange hole is semilocal and it strictly follows its reference electron, for relatively small $\omega$ values, the nonlocality of the exchange hole for this not-very-short-ranged electron-electron exchange interaction should still be important, and may not be adequately captured by SR DFA exchange alone.

To remedy this, we argue that mixing with a small amount of the SR HF exchange should be helpful. Similar to Becke's adiabatic-connection argument[14] for mixing a fraction of HF exchange with DFT, mixing a small fraction of the SR HF exchange with the SR DFA exchange should also improve thermochemistry and provide the desired nonlocal correction to the SR exchange. Furthermore, this does not affect the already correct LR behavior of the LC hybrid functionals. Similar arguments for the importance of the SR HF exchange were also made in Ref. 47.

Hence, we propose the following expression for the LC hybrid functionals:

$$E_{\text{xc}}^{\text{LC-DFA}} = E_x^{\text{LR-HF}} + c_x E_x^{\text{SR-HF}} + E_x^{\text{SR-DFA}} + E_c^{\text{DFA}}, \tag{9}$$

where $E_x^{\text{SR-HF}}$ is the SR HF exchange,

$$E_x^{\text{SR-HF}} = -\frac{1}{2}\sum_\sigma \sum_{i,j}^{\text{occ.}} \int \int \psi_{i\sigma}^*(\mathbf{r}_1)\psi_{j\sigma}^*(\mathbf{r}_1)$$
$$\times \frac{\text{erfc}(\omega r_{12})}{r_{12}} \psi_{i\sigma}(\mathbf{r}_2)\psi_{j\sigma}(\mathbf{r}_2) d\mathbf{r}_1 d\mathbf{r}_2, \tag{10}$$

and $c_x$ is a fractional number to be determined.

## III. SYSTEMATIC OPTIMIZATION

From the above arguments, the key ingredient for a successful LC hybrid functional is to construct a generally accurate $E_x^{\text{SR-DFA}}$ that is compatible with the $E_c^{\text{DFA}}$, the fraction of $E_x^{\text{SR-HF}}$, and the full $E_x^{\text{LR-HF}}$. Since the optimal $\omega$ for LC hybrid scheme is expected to be small, the optimal form of $E_x^{\text{SR-DFA}}$ should be close to that of $E_x^{\text{DFA}}$. Therefore, a minor modification to $E_x^{\text{DFA}}$ may provide a good starting point for developing accurate $E_x^{\text{SR-DFA}}$.

Since the uniform electron gas (UEG) limit of SR exchange is believed to be the leading contribution to the SR DFA exchange, and cannot be satisfied by any $E_x^{\text{DFA}}$ (unless $\omega=0$), we remedy this by replacing the LSDA exchange energy density $e_{x\sigma}^{\text{LSDA}}(\rho_\sigma)$ with the SR-LSDA exchange energy density $e_{x\sigma}^{\text{SR-LSDA}}(\rho_\sigma)$ [in Eq. (6)], while retaining its enhancement factor (gradient-corrected terms). In general, the enhancement factor of the SR-DFA exchange should be $\omega$-dependent, as the second-order gradient expansion of SR exchange depends on $\omega$.[33] For a sufficiently small $\omega$ value, however, our proposed functional form should be a good approximation.

To achieve a flexible functional form to represent the SR DFA exchange, we modify the B97 exchange functional[20] by replacing $e_{x\sigma}^{\text{LSDA}}(\rho_\sigma)$ with $e_{x\sigma}^{\text{SR-LSDA}}(\rho_\sigma)$ [in Eq. (6)], and denote this functional as SR-B97 (short-range B97) exchange, as it reduces to the B97 exchange functional at $\omega=0$.

$$E_x^{\text{SR-B97}} = \sum_\sigma \int e_{x\sigma}^{\text{SR-LSDA}}(\rho_\sigma) g_{x\sigma}(s_\sigma^2) d\mathbf{r}, \tag{11}$$

$$g_{x\sigma}(s_\sigma^2) = \sum_{i=0}^m c_{x\sigma,i} u_{x\sigma}^i, \tag{12}$$

where $g_{x\sigma}(s_\sigma^2)$ is a dimensionless inhomogeneity correction factor depending on the dimensionless reduced spin density gradient $s_\sigma = |\nabla\rho_\sigma|/\rho_\sigma^{4/3}$, and the expansion function $u_{x\sigma}$,

$$u_{x\sigma} = \gamma_{x\sigma} s_\sigma^2/(1 + \gamma_{x\sigma} s_\sigma^2), \tag{13}$$

$$\gamma_{x\sigma} = 0.004. \tag{14}$$

We use the same form for the correlation functional as the B97 correlation functional, which can be decomposed into same-spin $E_{c\sigma\sigma}^{\text{B97}}$ and opposite-spin $E_{c\alpha\beta}^{\text{B97}}$ components,

$$E_c^{\text{B97}} = \sum_\sigma E_{c\sigma\sigma}^{\text{B97}} + E_{c\alpha\beta}^{\text{B97}}. \tag{15}$$

For the same-spin terms,

$$E_{c\sigma\sigma}^{\mathrm{B97}} = \int e_{c\sigma\sigma}^{\mathrm{LSDA}}(\rho_\sigma) g_{c\sigma\sigma}(s_\sigma^2) d\mathbf{r}, \tag{16}$$

$$g_{c\sigma\sigma}(s_\sigma^2) = \sum_{i=0}^{m} c_{c\sigma\sigma,i} u_{c\sigma\sigma}^i, \tag{17}$$

$$u_{c\sigma\sigma} = \gamma_{c\sigma\sigma} s_\sigma^2 / (1 + \gamma_{c\sigma\sigma} s_\sigma^2), \tag{18}$$

$$\gamma_{c\sigma\sigma} = 0.2, \tag{19}$$

and for the opposite-spin terms,

$$E_{c\alpha\beta}^{\mathrm{B97}} = \int e_{c\alpha\beta}^{\mathrm{LSDA}}(\rho_\alpha,\rho_\beta) g_{c\alpha\beta}(s_{\mathrm{av}}^2) d\mathbf{r}, \tag{20}$$

$$g_{c\alpha\beta}(s_{\mathrm{av}}^2) = \sum_{i=0}^{m} c_{c\alpha\beta,i} u_{c\alpha\beta}^i, \tag{21}$$

$$u_{c\alpha\beta} = \gamma_{c\alpha\beta} s_{\mathrm{av}}^2 / (1 + \gamma_{c\alpha\beta} s_{\mathrm{av}}^2), \tag{22}$$

$$\gamma_{c\alpha\beta} = 0.006, \tag{23}$$

$$s_{\mathrm{av}}^2 = \tfrac{1}{2}(s_\alpha^2 + s_\beta^2). \tag{24}$$

The correlation energy densities $e_{c\sigma\sigma}^{\mathrm{LSDA}}$ and $e_{c\alpha\beta}^{\mathrm{LSDA}}$ are derived from Perdew–Wang[48] parametrization of the LSDA correlation energy, using the approach of Stoll *et al.*,[49]

$$e_{c\sigma\sigma}^{\mathrm{LSDA}}(\rho_\sigma) = e_c^{\mathrm{LSDA}}(\rho_\sigma,0), \tag{25}$$

$$e_{c\alpha\beta}^{\mathrm{LSDA}}(\rho_\alpha,\rho_\beta) = e_c^{\mathrm{LSDA}}(\rho_\alpha,\rho_\beta) - e_c^{\mathrm{LSDA}}(\rho_\alpha,0) \\ - e_c^{\mathrm{LSDA}}(0,\rho_\beta). \tag{26}$$

Based on the above functional expansions, we propose two new LC hybrid functionals, $\omega$B97 and $\omega$B97X. $\omega$B97 has no SR HF exchange (like most of the LC hybrid functionals),

$$E_{\mathrm{xc}}^{\omega\mathrm{B97}} = E_x^{\mathrm{LR\text{-}HF}} + E_x^{\mathrm{SR\text{-}B97}} + E_c^{\mathrm{B97}}. \tag{27}$$

By contrast, $\omega$B97X contains a small fraction of the SR HF exchange (the "X" stands for the use of the SR HF exchange),

$$E_{\mathrm{xc}}^{\omega\mathrm{B97X}} = E_x^{\mathrm{LR\text{-}HF}} + c_x E_x^{\mathrm{SR\text{-}HF}} + E_x^{\mathrm{SR\text{-}B97}} + E_c^{\mathrm{B97}}. \tag{28}$$

We determined the optimal $\omega$ values, the linear expansion coefficients, the expansion order $m$ of $E_{\mathrm{xc}}^{\omega\mathrm{B97}}$ and $E_{\mathrm{xc}}^{\omega\mathrm{B97X}}$ by least-squares fittings to 412 accurate experimental and accurate theoretical results (the training set), including the 18 atomic energies from the H atom to the Ar atom,[50] the atomization energies of the G3/99 set[51–53] (223 molecules), the ionization potentials (IPs) of the G2-1 set[54] [40 molecules, excluding $SH_2$ ($^2A_1$) and $N_2$ ($^2\Pi$) cations due to the known convergence problems for pure density functionals[52]], the electron affinities (EAs) of the G2-1 set (25 molecules), the proton affinities (PAs) of the G2-1 set (8 molecules), the 76 barrier heights of the NHTBH38/04 and HTBH38/04 sets,[55,56] and the 22 noncovalent interactions of the S22 set.[57] All data are equally weighted in the least-squares fitting. By

choosing a diverse range of training data, our goal is to achieve optimized functionals whose performance is well-balanced across typical applications.

We enforce the exact UEG limit for the $\omega$B97 and $\omega$B97X functionals by imposing the following constraints:

$$c_{c\sigma\sigma,0} = 1, \tag{29}$$

$$c_{c\alpha\beta,0} = 1, \tag{30}$$

$$c_{x\sigma,0} = 1, \quad \text{for } E_{\mathrm{xc}}^{\omega\mathrm{B97}}, \tag{31}$$

and

$$c_{x\sigma,0} + c_x = 1, \quad \text{for } E_{\mathrm{xc}}^{\omega\mathrm{B97X}}. \tag{32}$$

Searching for the optimal parameters for $\omega$B97 and $\omega$B97X naively seems impractical due to the use of large number of empirical parameters. Following Van Voorhis and Scuseria,[21] our parameters are obtained by an iterative procedure. First, we focus on a limited range of possible $\omega$ values between 0.0 and 0.5 bohr$^{-1}$ based on those studied in previous LC hybrid functionals. For each $\omega$ value (0.0, 0.1, 0.2, 0.3, 0.4, or 0.5 bohr$^{-1}$), the corresponding RSHXLDA orbitals[39] are used as the initial guess orbitals for least-squares fitting. We then obtain, for each $\omega$ value, a new set of linear expansion coefficients. With this new set of linear expansion coefficients, the corresponding self-consistent orbitals can be obtained and then used for another least-squares fitting. This procedure is repeated, for each $\omega$ value, until the energies and the linear expansion coefficients are sufficiently close to the previous ones.

Interestingly, we have found that the statistical errors obtained in the first cycle (using the RSHXLDA orbitals) are not very different from those obtained self-consistently, even though the linear expansion coefficients in different iterative cycles can be different. This indicates that one could have a good estimate of the performance of proposed functionals, for each $\omega$ value, even in its first iterative cycle (this is some-

TABLE I. Optimized parameters for the $\omega$B97 [in Eq. (27)], and $\omega$B97X [in Eq. (28)].

|  | $\omega$B97 | $\omega$B97X |
|---|---|---|
| $\omega$ | 0.4 bohr$^{-1}$ | 0.3 bohr$^{-1}$ |
| $c_{x\sigma,0}$ | $1.00000E+00$ | $8.42294E-01$ |
| $c_{c\sigma\sigma,0}$ | $1.00000E+00$ | $1.00000E+00$ |
| $c_{c\alpha\beta,0}$ | $1.00000E+00$ | $1.00000E+00$ |
| $c_{x\sigma,1}$ | $1.13116E+00$ | $7.26479E-01$ |
| $c_{c\sigma\sigma,1}$ | $-2.55352E+00$ | $-4.33879E+00$ |
| $c_{c\alpha\beta,1}$ | $3.99051E+00$ | $2.37031E+00$ |
| $c_{x\sigma,2}$ | $-2.74915E+00$ | $1.04760E+00$ |
| $c_{c\sigma\sigma,2}$ | $1.18926E+01$ | $1.82308E+01$ |
| $c_{c\alpha\beta,2}$ | $-1.70066E+01$ | $-1.13995E+01$ |
| $c_{x\sigma,3}$ | $1.20900E+01$ | $-5.70635E+00$ |
| $c_{c\sigma\sigma,3}$ | $-2.69452E+01$ | $-3.17430E+01$ |
| $c_{c\alpha\beta,3}$ | $1.07292E+00$ | $6.58405E+00$ |
| $c_{x\sigma,4}$ | $-5.71642E+00$ | $1.32794E+01$ |
| $c_{c\sigma\sigma,4}$ | $1.70927E+01$ | $1.72901E+01$ |
| $c_{c\alpha\beta,4}$ | $8.88211E+00$ | $-3.78132E+00$ |
| $c_x$ |  | $1.57706E-01$ |

TABLE II. Statistical errors (in kcal/mol) of the training set, including atomization energies (AEs) of the G3/99 set (233 molecules) (Refs. 51–53 and 61), ionization potentials (IPs) of the G2-1 set [40 molecules, except for SH$_2$ ($^2A_1$) and N$_2$ ($^2\Pi$) cations], electron affinities (EAs) of the G2-1 set (25 molecules), proton affinities (PAs) of the G2-1 set (8 molecules) (Ref. 54), nonhydrogen transfer barrier heights of the NHTBH38/04 set (38 barrier heights), hydrogen transfer barrier heights of the HTBH38/04 set (38 barrier heights) (Refs. 55 and 56), and the S22 set (22 molecules) for noncovalent interactions (Ref. 57). The B97* and HCTH* functionals are defined in the text. For all cases, single-point calculations are performed using the 6-311++G(3$df$,3$pd$) basis set. For the AE, IP, EA, and PA, the geometries and zero-point energies were obtained at the B3LYP/6-31G(2$df$,$p$) level using a frequency scale factor of 0.9854 for zero-point energies. For the AE, the scaled (0.9854) thermal correction at the B3LYP/6-31G(2$df$,$p$) level and experimental spin-orbit corrections for the atoms are also used for reversely converting experimental enthalpies of formation to atomization energies. For the S22 set, counterpoise corrections are used to reduce basis set superposition errors, and monomer deformations are not included in the interaction energies.

| System | Error | $\omega$B97X | $\omega$B97 | B97* | HCTH* | B97-1 | B3LYP | BLYP |
|---|---|---|---|---|---|---|---|---|
| | MSE | −0.09 | −0.20 | 0.54 | 1.74 | −1.58 | −4.30 | −4.60 |
| G3/99 (223) | MAE | 2.09 | 2.56 | 2.99 | 4.80 | 4.85 | 5.46 | 9.77 |
| | rms | 2.86 | 3.51 | 4.19 | 6.27 | 6.32 | 7.35 | 12.97 |
| | MSE | −0.15 | −0.48 | 2.33 | 0.37 | −0.29 | 2.16 | −1.51 |
| IP (40) | MAE | 2.69 | 2.65 | 3.45 | 3.70 | 2.60 | 3.68 | 4.42 |
| | rms | 3.59 | 3.58 | 4.59 | 4.49 | 3.22 | 4.80 | 5.27 |
| | MSE | −0.43 | −1.45 | 1.03 | 1.71 | −0.90 | 1.73 | 0.39 |
| EA (25) | MAE | 2.05 | 2.67 | 2.46 | 2.60 | 1.95 | 2.39 | 2.58 |
| | rms | 2.59 | 3.10 | 3.25 | 3.73 | 2.42 | 3.31 | 3.20 |
| | MSE | 0.60 | 0.68 | −0.69 | 1.31 | 0.62 | −0.75 | −1.45 |
| PA (8) | MAE | 1.22 | 1.45 | 1.23 | 1.77 | 0.99 | 1.14 | 1.57 |
| | rms | 1.72 | 2.17 | 1.32 | 2.27 | 1.52 | 1.35 | 2.10 |
| | MSE | 0.56 | 1.32 | −2.21 | −6.35 | −3.14 | −4.57 | −8.68 |
| NHTBH (38) | MAE | 1.75 | 2.31 | 2.67 | 6.70 | 3.52 | 4.69 | 8.72 |
| | rms | 2.08 | 2.82 | 3.41 | 8.18 | 4.26 | 5.71 | 10.26 |
| | MSE | −1.51 | −0.34 | −2.73 | −6.25 | −4.76 | −4.48 | −7.84 |
| HTBH (38) | MAE | 2.24 | 2.24 | 2.89 | 6.34 | 4.76 | 4.56 | 7.84 |
| | rms | 2.58 | 2.62 | 3.18 | 7.16 | 5.39 | 5.10 | 8.66 |
| | MSE | 0.53 | 0.16 | 2.64 | 4.96 | 2.55 | 3.94 | 5.04 |
| S22 (22) | MAE | 0.87 | 0.60 | 2.69 | 4.96 | 2.55 | 3.94 | 5.04 |
| | rms | 1.30 | 0.80 | 4.06 | 6.03 | 3.60 | 5.16 | 6.29 |
| | MSE | −0.15 | −0.14 | 0.27 | 0.22 | −1.58 | −2.77 | −4.07 |
| All (394) | MAE | 2.05 | 2.39 | 2.91 | 4.83 | 4.10 | 4.75 | 8.05 |
| | rms | 2.75 | 3.23 | 3.98 | 6.22 | 5.42 | 6.39 | 10.88 |

thing we shall employ in assessing the usefulness of the new functional forms). All of the self-consistent optimizations are well converged within four iterative cycles.

During the optimization procedure, we found that the statistical errors are not significantly improved for $m > 4$. Thus, the functional expansions employed in $\omega$B97 and $\omega$B97X are truncated at $m = 4$. For $\omega$B97, the range separator $\omega = 0.4$ bohr$^{-1}$ is found to be optimal, which is the same result found by Vydrov et al.[41,42] and in agreement with recent arguments made by Fromager et al.[58] However, a slightly smaller optimal value, $\omega = 0.3$ bohr$^{-1}$, is found for $\omega$B97X. As might be anticipated, the presence of a small fraction of the (nonlocal) SR HF exchange allows the SR part to be longer ranged. The optimized parameters of the $\omega$B97 and $\omega$B97X functionals are given in Table I.

The limiting cases where $\omega = 0$ for $\omega$B97X and $\omega$B97 are especially interesting, as these reduce to the same functional forms as the existing B97 (Ref. 20) and HCTH (Ref. 22)

functionals, respectively. Therefore, it is important to know how well B97 and HCTH perform here, when they are both optimized on the same training set. We thus reoptimize B97 and HCTH functionals on the same training set, truncate their functional expansions at the same order $m = 4$, and impose the same UEG limit. Their optimizations are done in a post-LSDA manner (LSDA orbitals are used for the linear least-squares fittings, instead of using their self-consistent orbitals). As mentioned above, these post-LSDA results are believed to be quite close to the fully optimized self-consistent results. For comparisons within the training set, we denote these two reoptimized functionals as B97* and HCTH*, respectively.

## IV. RESULTS FOR THE TRAINING SET

All calculations are performed with a development version of Q-CHEM 3.0.[59] Spin-restricted theory is used for singlet

states and spin-unrestricted theory for others, unless noted otherwise. Results for the training set are computed using the 6-311++G($3df$,$3pd$) basis set with the SG-1 grid[60] for numerically integrating the exchange-correlation contributions. As is usual in hybrid density functional approaches, the electronic energy is minimized with respect to the orbitals. The overall performance of the two new LC hybrid functionals is compared with B97*, HCTH*, B97-1,[22] B3LYP,[14,16] and BLYP (Refs. 17 and 18) in Table II. The first two comparisons are particularly significant because they indicate how much improvement is possible with the addition of a single extra parameter corresponding to making long-range exchange exact and thus self-interaction free. The comparisons with other functionals that are not optimized on the same training set are interesting but not as significant as the comparisons on independent test sets discussed later.

The error for each entry is defined as (error = theoretical value − reference value). The notation used for characterizing statistical errors is as follows: Mean signed errors (MSEs), mean absolute errors (MAEs), root-mean-square (rms) errors, maximum negative errors (Max(−)), and maximum positive errors (Max(+)).

## A. Thermochemistry

Satisfactory accuracy for thermochemical calculations is one major criterion to judge the performance of density functionals. The G3/99 set,[51–53] compiled by Curtiss et al., is probably the leading standard test set for this purpose. Following the procedure of G3X theory,[61] the optimized B3LYP/6-31G($2df$,$p$) geometries and zero-point energies are used for all species. A frequency scale factor of 0.9854 is used for zero-point energies and thermal corrections,[61] and atomic spin-orbital effects (corrected by experimental results[51]) are included. Enthalpies of formation of free atoms are taken from experiment.[51] The experimental atomization energies are then obtained from experimental standard enthalpies of formation (at 298 K) with a reverse application of G3X theory.[61]

The IPs, EAs, and PAs of the G2-1 set[54] are determined at zero temperature and atomic spin-orbit effects are not considered. As can be seen in Table II, $\omega$B97X, $\omega$B97, and B97* provide very accurate thermochemical results, especially atomization energies. Their performances on the IP, EA, and PA training sets are comparable. The important role of long-range exchange in obtaining good results can be clearly seen by comparing results for $\omega$B97 with HCTH*: These functionals differ by just one parameter (16 versus 15) but results are qualitatively improved. The addition of short-range exchange controlled by one more mixing parameter in $\omega$B97X leads to further improvements in the quality of results, which shows that this too is a physically important enhancement to the functional form.

In Table III, we compare the performance of various functionals on atomization energies of the G3/99 set. As can been seen, $\omega$B97X performs best, followed by $\omega$B97. Since the G3/99 set is part of the training set for $\omega$B97X and $\omega$B97, one cannot attach much significance to this result—it

TABLE III. Summary of performance of various functionals for the atomization energies (in kcal/mol) of the G3/99 set. The last two columns indicate whether the functionals are exact in the uniform electron gas (UEG) limit and are long-range corrected (LC) hybrid functionals. The results for the MCY1 and MCY2 are taken from Ref. 62, and the results for the BMK, M05-2X, and LC-$\omega$PBE PBE are taken from Ref. 42.

| Functional | MSE | MAE | UEG | LC |
|---|---|---|---|---|
| $\omega$B97X | −0.09 | 2.09 | Yes | Yes |
| $\omega$B97 | −0.20 | 2.56 | Yes | Yes |
| MCY1 | | 3.16 | No | Yes |
| MCY2 | | 3.37 | No | Yes |
| BMK | 2.68 | 3.69 | No | No |
| M05-2X | 2.84 | 4.16 | Yes | No |
| LC-$\omega$PBE | 0.93 | 4.25 | Yes | Yes |
| B97-1 | −1.58 | 4.85 | No | No |
| B3LYP | −4.30 | 5.46 | No | No |

is a necessary but not sufficient indication of their potential usefulness. MCY1, MCY2,[62] and BMK (Ref. 15) perform reasonably well on this test set, while M05-2X,[27] LC-$\omega$PBE,[41,42] and B97-1 (Ref. 22) provide only slight improvement over the most popular hybrid functional, B3LYP.[14,16] The last two columns in Table III tell whether the functionals obey the exact UEG limit, and whether they are LC hybrid functionals.

## B. Kinetics

We evaluate the performance of functionals for barrier heights of chemical reactions in the NHTBH38/04 and HTBH38/04 sets.[55,56] The NHTBH38/04 set contains both forward and reverse barrier heights for 19 non-hydrogen-transfer reactions, and the HTBH38/04 set contains both forward and reverse barrier heights for 19 hydrogen-transfer reactions. The optimized geometries and the reference energies are taken from Refs. 55 and 56. As can be seen in Table II, $\omega$B97X, $\omega$B97, and B97* provide accurate kinetics, compared to HCTH*, B97-1, B3LYP, and BLYP. It is noticeable that the pure density functional, HCTH*, severely underestimates the barrier heights due to self-interaction errors, despite these data being part of its training set. Furthermore, the full inclusion of long-range exact exchange in $\omega$B97X and $\omega$B97 improves results relative to B97*, showing that it is important for improving reaction barriers. Detailed informations for the performance of functionals on these two sets are also given in Tables IV and V.

## C. Noncovalent interactions

For noncovalent complexes in the S22 set,[57] we perform calculations with the usual counterpoise corrections[63] for reducing the basis set superposition error (BSSEs). Monomer deformation energies are not included. In Table II, we observe that all the functionals predict underbinding results, except for $\omega$B97X and $\omega$B97. Clearly, B97* and HCTH* fail for noncovalent interactions, even though these data are included in their training set. This indicates that there is limited scope to simultaneously improve thermochemistry, kinetics, and noncovalent interactions by reoptimizing the parameters for B97 and HCTH. By contrast, inclusion of exact long-

TABLE IV. Nonhydrogen transfer barrier heights (in kcal/mol) of the NHTBH38/04 set (Ref. 56).

| Reactions | | $\Delta E_{ref}$ | $\omega$B97X | $\omega$B97 | B97-1 | B3LYP | BLYP |
|---|---|---|---|---|---|---|---|
| Heavy-atom transfer reactions | | | | | | | |
| $H+N_2O \rightarrow OH+N_2$ | $V^f$ | 18.14 | 19.22 | 20.67 | 15.89 | 11.36 | 8.53 |
| | $V^r$ | 83.22 | 80.57 | 81.93 | 72.49 | 72.81 | 61.66 |
| $H+FH \rightarrow HF+H$ | $V^f$ | 42.18 | 43.10 | 44.78 | 37.93 | 31.01 | 26.03 |
| | $V^r$ | 42.18 | 43.10 | 44.78 | 37.93 | 31.01 | 26.03 |
| $H+ClH \rightarrow HCl+H$ | $V^f$ | 18.00 | 20.73 | 23.17 | 16.23 | 12.42 | 9.81 |
| | $V^r$ | 18.00 | 20.73 | 23.17 | 16.23 | 12.42 | 9.81 |
| $H+FCH_3 \rightarrow HF+CH_3$ | $V^f$ | 30.38 | 32.14 | 33.46 | 27.55 | 21.78 | 16.11 |
| | $V^r$ | 57.02 | 55.41 | 55.83 | 49.63 | 48.63 | 42.27 |
| $H+F_2 \rightarrow HF+F$ | $V^f$ | 2.27 | 0.86 | 1.96 | −2.36 | −7.54 | −11.67 |
| | $V^r$ | 106.18 | 104.27 | 103.66 | 98.12 | 96.17 | 82.16 |
| $CH_3+FCl \rightarrow CH_3F+Cl$ | $V^f$ | 7.43 | 3.93 | 4.62 | −2.15 | −1.56 | −6.95 |
| | $V^r$ | 60.17 | 58.52 | 59.96 | 51.22 | 51.08 | 41.90 |
| Nucleophilic substitution reactions | | | | | | | |
| $F^- + CH_3F \rightarrow FCH_3 + F^-$ | $V^f$ | −0.34 | −2.27 | −2.60 | −3.74 | −3.93 | −7.90 |
| | $V^r$ | −0.34 | −2.27 | −2.60 | −3.74 | −3.93 | −7.90 |
| $F^- \cdots CH_3F \rightarrow FCH_3 \cdots F^-$ | $V^f$ | 13.38 | 13.28 | 13.32 | 10.82 | 10.21 | 6.47 |
| | $V^r$ | 13.38 | 13.28 | 13.32 | 10.82 | 10.21 | 6.47 |
| $Cl^- + CH_3Cl \rightarrow ClCH_3 + Cl^-$ | $V^f$ | 3.10 | 4.71 | 6.21 | −1.03 | −0.57 | −3.96 |
| | $V^r$ | 3.10 | 4.71 | 6.21 | −1.03 | −0.57 | −3.96 |
| $Cl^- \cdots CH_3Cl \rightarrow ClCH_3 \cdots Cl^-$ | $V^f$ | 13.61 | 16.09 | 17.74 | 9.90 | 9.30 | 5.81 |
| | $V^r$ | 13.61 | 16.09 | 17.74 | 9.90 | 9.30 | 5.81 |
| $F^- + CH_3Cl \rightarrow FCH_3 + Cl^-$ | $V^f$ | −12.54 | −13.11 | −11.72 | −17.00 | −16.57 | −19.37 |
| | $V^r$ | 20.11 | 20.83 | 20.15 | 17.99 | 18.25 | 13.02 |
| $F^- \cdots CH_3Cl \rightarrow FCH_3 \cdots Cl^-$ | $V^f$ | 2.89 | 4.23 | 5.39 | 0.68 | 0.29 | −1.68 |
| | $V^r$ | 29.62 | 31.19 | 30.95 | 27.20 | 26.68 | 21.09 |
| $OH^- + CH_3F \rightarrow HOCH_3 + F^-$ | $V^f$ | −2.78 | −3.70 | −4.05 | −5.94 | −5.83 | −9.78 |
| | $V^r$ | 17.33 | 17.64 | 17.86 | 14.36 | 14.14 | 9.08 |
| $OH^- \cdots CH_3F \rightarrow HOCH_3 \cdots F^-$ | $V^f$ | 10.96 | 11.47 | 11.52 | 8.11 | 7.69 | 3.73 |
| | $V^r$ | 47.20 | 49.33 | 49.13 | 46.44 | 45.46 | 40.23 |
| Unimolecular and association reactions | | | | | | | |
| $H+N_2 \rightarrow HN_2$ | $V^f$ | 14.69 | 13.99 | 15.47 | 11.24 | 7.47 | 5.25 |
| | $V^r$ | 10.72 | 14.32 | 15.06 | 12.39 | 10.87 | 8.50 |
| $H+CO \rightarrow HCO$ | $V^f$ | 3.17 | 4.55 | 5.65 | 3.08 | −0.60 | −1.96 |
| | $V^r$ | 22.68 | 26.72 | 27.07 | 25.40 | 24.60 | 23.34 |
| $H+C_2H_4 \rightarrow CH_3CH_2$ | $V^f$ | 1.72 | 4.07 | 4.94 | 3.23 | −0.22 | −0.74 |
| | $V^r$ | 41.75 | 47.07 | 48.49 | 43.14 | 41.71 | 38.08 |
| $CH_3+C_2H_4 \rightarrow CH_3CH_2CH_2$ | $V^f$ | 6.85 | 5.04 | 4.81 | 3.35 | 5.97 | 4.70 |
| | $V^r$ | 32.97 | 35.21 | 36.59 | 31.00 | 29.41 | 24.85 |
| $HCN \rightarrow HCN$ | $V^f$ | 48.16 | 46.29 | 45.89 | 46.07 | 47.39 | 46.77 |
| | $V^r$ | 33.11 | 33.12 | 32.80 | 32.71 | 33.33 | 31.69 |
| MSE | | | 0.56 | 1.32 | −3.14 | −4.57 | −8.68 |
| MAE | | | 1.75 | 2.31 | 3.52 | 4.69 | 8.72 |
| rms | | | 2.08 | 2.82 | 4.26 | 5.71 | 10.26 |
| Max(−) | | | −3.50 | −2.81 | −10.73 | −11.17 | −24.02 |
| Max(+) | | | 5.32 | 6.74 | 2.72 | 1.92 | 0.66 |

range exchange in $\omega$B97X and $\omega$B97 leads to significant improvement. Detailed information on the S22 set can been seen in Table VI. This shows that B97-1, B3LYP, and BLYP are all underbinding, and completely fail for dispersion-bound complexes, while $\omega$B97X and $\omega$B97 are still doing a reasonable (though not highly accurate) job.

## V. RESULTS FOR THE TEST SETS

To test the *transferability* of the performance of the two new LC hybrid functionals, we evaluate their performance outside their training sets and compare the results with other three widely used functionals, B97-1,[22] B3LYP,[14,16] and BLYP.[17,18] Calculations are performed on various test sets

involving 48 atomization energies, 30 reaction energies, 29 noncovalent interactions, 166 optimized geometry properties, four dissociation curves of symmetric radical cations, and one long-range charge-transfer excitation curve of two well-separated molecules. There are a total of 278 pieces of data in the test sets.

## A. Atomization energies

The additional 48 atomization energies in the G3/05 test set[64] (other than the 223 atomization energies in the G3/99 test set[51–53]) are computed by various density functionals. This test set can be regarded as one of the most stringent test sets, as it contains third-row elements (none is in our training

TABLE V. Hydrogen transfer barrier heights (in kcal/mol) of the HTBH38/04 set (Ref. 55 and 56).

| Reactions | | $\Delta E_{ref}$ | $\omega$B97X | $\omega$B97 | B97-1 | B3LYP | BLYP |
|---|---|---|---|---|---|---|---|
| H+HCl→H$_2$+Cl | $V^f$ | 5.7 | 5.33 | 6.68 | 2.95 | −0.78 | −2.47 |
| | $V^r$ | 8.7 | 5.24 | 6.49 | 2.33 | 3.71 | 1.81 |
| OH+H$_2$→H+H$_2$O | $V^f$ | 5.1 | 2.56 | 3.27 | −0.03 | 0.51 | −3.50 |
| | $V^r$ | 21.2 | 19.50 | 20.39 | 17.69 | 13.35 | 10.38 |
| CH$_3$+H$_2$→H+CH$_4$ | $V^f$ | 12.1 | 9.63 | 10.29 | 7.04 | 8.73 | 7.14 |
| | $V^r$ | 15.3 | 15.13 | 16.35 | 13.21 | 9.52 | 7.64 |
| OH+CH$_4$→CH$_3$+H$_2$O | $V^f$ | 6.7 | 3.97 | 4.53 | 0.60 | 1.92 | −2.75 |
| | $V^r$ | 19.6 | 15.41 | 15.59 | 12.15 | 13.97 | 10.63 |
| H+H$_2$→H$_2$+H | $V^f$ | 9.6 | 10.74 | 12.38 | 8.92 | 4.22 | 2.86 |
| | $V^r$ | 9.6 | 10.74 | 12.38 | 8.92 | 4.22 | 2.86 |
| OH+NH$_3$→H$_2$O+NH$_2$ | $V^f$ | 3.2 | 1.62 | 2.83 | −3.75 | −2.63 | −9.21 |
| | $V^r$ | 12.7 | 10.97 | 12.10 | 6.03 | 7.31 | 1.81 |
| HCl+CH$_3$→Cl+CH$_4$ | $V^f$ | 1.7 | −1.07 | −0.47 | −4.22 | −1.57 | −3.48 |
| | $V^r$ | 7.9 | 4.34 | 5.41 | 1.33 | 3.71 | 1.30 |
| OH+C$_2$H$_6$→H$_2$O+C$_2$H$_5$ | $V^f$ | 3.4 | 1.26 | 1.85 | −2.34 | −1.08 | −6.15 |
| | $V^r$ | 19.9 | 17.22 | 17.31 | 14.08 | 15.61 | 12.33 |
| F+H$_2$→HF+H | $V^f$ | 1.8 | −3.89 | −3.76 | −5.88 | −6.03 | −11.62 |
| | $V^r$ | 33.4 | 29.17 | 29.80 | 28.10 | 23.76 | 20.70 |
| O+CH$_4$→OH+CH$_3$ | $V^f$ | 13.7 | 9.94 | 10.45 | 6.04 | 6.78 | 1.43 |
| | $V^r$ | 8.1 | 4.85 | 4.82 | 1.98 | 4.44 | 1.67 |
| H+PH$_3$→PH$_2$+H$_2$ | $V^f$ | 3.1 | 4.62 | 5.88 | 2.87 | −1.04 | −2.56 |
| | $V^r$ | 23.2 | 24.11 | 25.25 | 21.83 | 22.71 | 21.57 |
| H+HO→H$_2$+O | $V^f$ | 10.7 | 9.79 | 10.68 | 7.89 | 4.14 | 1.60 |
| | $V^r$ | 13.1 | 9.38 | 10.26 | 5.78 | 5.69 | 0.86 |
| H+H$_2$S→H$_2$+HS | $V^f$ | 3.5 | 5.54 | 6.94 | 3.26 | −0.55 | −2.16 |
| | $V^r$ | 17.3 | 17.16 | 18.42 | 14.49 | 15.59 | 14.06 |
| O+HCl→OH+Cl | $V^f$ | 9.8 | 7.07 | 14.21 | −0.14 | 0.99 | −8.73 |
| | $V^r$ | 10.4 | 7.38 | 14.45 | 1.36 | 3.94 | −3.71 |
| NH$_2$+CH$_3$→CH$_4$+NH | $V^f$ | 8.0 | 6.50 | 6.95 | 3.21 | 6.12 | 3.56 |
| | $V^r$ | 22.4 | 19.42 | 20.07 | 15.57 | 17.08 | 13.31 |
| NH$_2$+C$_2$H$_5$→C$_2$H$_6$+NH | $V^f$ | 7.5 | 8.48 | 8.82 | 5.36 | 8.18 | 5.92 |
| | $V^r$ | 18.3 | 16.87 | 17.54 | 12.84 | 14.51 | 10.56 |
| C$_2$H$_6$+NH$_2$→NH$_3$+C$_2$H$_5$ | $V^f$ | 10.4 | 10.16 | 11.01 | 6.40 | 8.70 | 5.21 |
| | $V^r$ | 17.4 | 16.77 | 17.21 | 13.05 | 15.44 | 12.69 |
| NH$_2$+CH$_4$→CH$_3$+NH$_3$ | $V^f$ | 14.5 | 12.64 | 13.49 | 9.05 | 11.26 | 7.98 |
| | $V^r$ | 17.8 | 14.72 | 15.29 | 10.82 | 13.38 | 10.34 |
| *s-trans cis*-C$_5$H$_8$→*s-trans cis*-C$_5$H$_8$ | $V^f$ | 38.4 | 41.44 | 42.84 | 36.90 | 38.79 | 35.84 |
| | $V^r$ | 38.4 | 41.44 | 42.84 | 36.90 | 38.79 | 35.84 |
| MSE | | | −1.51 | −0.34 | −4.76 | −4.48 | −7.84 |
| MAE | | | 2.24 | 2.24 | 4.76 | 4.56 | 7.84 |
| rms | | | 2.58 | 2.62 | 5.39 | 5.10 | 8.66 |
| Max(−) | | | −5.69 | −5.56 | −9.94 | −9.64 | −18.53 |
| Max(+) | | | 3.04 | 4.44 | −0.23 | 0.68 | −1.58 |

set), and the accuracy of density functionals for atomization energies is usually very sensitive to their functional forms. Following G4 theory,[65] the equilibrium structure is obtained by B3LYP with the 6-31G($2df,p$) basis set for the first two row atoms, and the 6-31G($2fg$) (Ref. 65) for the third-row nontransition metal elements. The same equilibrium structure is used to obtain harmonic frequencies and thermal corrections, which are then both scaled by a factor of 0.9854. Atomic spin-orbit corrections are also included.[65] Enthalpies of formation of free atoms are taken from experiment.[51,66] For single-point calculations, the G3LargeXP basis set defined in Ref. 65 is used, with the extra fine grid, EML(99,590), consisting of 99 Euler–Maclaurin radial grid points[67] and 590 Lebedev angular grid points.[68] As can be

seen in Table VII, $\omega$B97X performs best and is noticeably better than $\omega$B97, which supports the importance of the SR HF exchange for thermochemistry. BLYP, in particular, produces large average deviations for this test set.

## B. Reaction energies

The reaction energies of 30 chemical reactions are taken from the NHTBH38/04 and HTBH38/04 databases. These are the reactions with different barrier heights for the forward and backward directions. The reaction energies are obtained by taking the differences of these barrier heights. Results are computed using the 6-311++G($3df,3pd$) basis set with the SG-1 grid.[60] As can be seen in Table VIII, all hybrid

TABLE VI. Interaction energies (in kcal/mol) for the S22 set (Ref. 57). The conterpoise corrections are used to reduce the basis set superposition errors. Monomer deformation energies are not included.

| Complex [Symmetry] | $\Delta E_{ref}$ | $\omega$B97X | $\omega$B97 | B97-1 | B3LYP | BLYP |
|---|---|---|---|---|---|---|
| Hydrogen-bonded complexes | | | | | | |
| $(NH_3)_2$ $[C_{2h}]$ | −3.17 | −3.58 | −3.64 | −2.85 | −2.19 | −1.78 |
| $(H_2O)_2$ $[C_s]$ | −5.02 | −5.59 | −5.64 | −4.88 | −4.49 | −3.99 |
| Formic acid dimer $[C_{2h}]$ | −18.61 | −19.96 | −20.13 | −17.94 | −17.29 | −15.48 |
| Formamide dimer $[C_{2h}]$ | −15.96 | −16.65 | −16.78 | −14.78 | −13.97 | −12.44 |
| Uracil dimer $[C_{2h}]$ | −20.65 | −20.30 | −20.31 | −18.60 | −17.88 | −16.22 |
| 2-pyridoxine·2-aminopyridine $[C_1]$ | −16.71 | −16.37 | −16.40 | −14.82 | −13.72 | −12.51 |
| Adenine·thymine WC $[C_1]$ | −16.37 | −15.91 | −16.05 | −14.07 | −12.82 | −11.41 |
| MSE | | −0.27 | −0.35 | 1.22 | 2.02 | 3.24 |
| MAE | | 0.60 | 0.63 | 1.22 | 2.02 | 3.24 |
| Dispersion complexes | | | | | | |
| $(CH_4)_2$ $[D_{3d}]$ | −0.53 | −0.57 | −0.44 | −0.22 | 0.40 | 0.68 |
| $(C_2H_4)_2$ $[D_{2d}]$ | −1.51 | −1.77 | −1.92 | −0.60 | 0.52 | 1.13 |
| Benzene·CH$_4$ $[C_3]$ | −1.50 | −1.41 | −1.55 | −0.25 | 0.82 | 1.38 |
| Benzene dimer $[C_{2h}]$ | −2.73 | −1.57 | −2.33 | 1.56 | 3.85 | 4.95 |
| Pyrazine dimer $[C_s]$ | −4.42 | −2.86 | −3.68 | 0.37 | 2.53 | 3.75 |
| Uracil dimer $[C_2]$ | −10.12 | −7.84 | −8.90 | −3.52 | −0.87 | 1.14 |
| Indole·benzene $[C_1]$ | −5.22 | −2.39 | −3.58 | 1.90 | 4.78 | 6.27 |
| Adenine·thymine stack $[C_1]$ | −12.23 | −8.40 | −10.26 | −2.09 | 1.41 | 3.99 |
| MSE | | 1.43 | 0.70 | 4.42 | 6.46 | 7.69 |
| MAE | | 1.51 | 0.82 | 4.42 | 6.46 | 7.69 |
| Mixed complexes | | | | | | |
| Ethene·ethine $[C_{2v}]$ | −1.53 | −1.67 | −1.63 | −1.31 | −0.64 | −0.29 |
| Benzene·H$_2$O $[C_s]$ | −3.28 | −3.39 | −3.56 | −2.29 | −1.21 | −0.49 |
| Benzene·NH$_3$ $[C_s]$ | −2.35 | −2.31 | −2.46 | −1.17 | −0.09 | 0.55 |
| Benzene·HCN $[C_s]$ | −4.46 | −4.61 | −4.89 | −3.20 | −1.93 | −0.94 |
| Benzene dimer $[C_{2v}]$ | −2.74 | −2.11 | −2.38 | −0.38 | 1.03 | 1.87 |
| Indole·benzene T-shape $[C_1]$ | −5.73 | −4.44 | −4.82 | −2.35 | −0.50 | 0.68 |
| Phenol dimer $[C_1]$ | −7.05 | −6.49 | −6.93 | −4.21 | −2.94 | −1.75 |
| MSE | | 0.30 | 0.07 | 1.75 | 2.98 | 3.82 |
| MAE | | 0.42 | 0.33 | 1.75 | 2.98 | 3.82 |
| MSE | | 0.53 | 0.16 | 2.55 | 3.94 | 5.04 |
| MAE | | 0.87 | 0.60 | 2.55 | 3.94 | 5.04 |
| rms | | 1.30 | 0.80 | 3.60 | 5.16 | 6.29 |
| Max(−) | | −1.35 | −1.52 | 0.14 | 0.53 | 1.03 |
| Max(+) | | 3.83 | 1.97 | 10.14 | 13.64 | 16.22 |

functionals perform comparably. B97-1, B3LYP, and BLYP perform much better here than for the barrier heights of the same sets, which can be attributed to better cancelation of errors from the consistent underestimations of the barrier heights.

## C. Noncovalent interactions

The performances of various functionals are examined on several sets of noncovalent interactions. The first three sets are taken from Ref. 69, involving binding energies of seven charge-transfer complexes (the CT7/04 database), six dipole-dipole interaction complexes (the DI6/04 databse), and seven weak-interaction complexes (the WI7/05 database), where monomer deformation energies are included. The last three sets consist of the final three entries of the hydrogen-bonded DNA base pairs, interstrand base pairs, and stacked base pairs of Ref. 57, where monomer deformation energies are not considered. The 6-311++G($3df,3pd$) basis

TABLE VII. Statistical errors of the additional 48 atomization energies in the G3/05 set (Ref. 64).

| Error | $\omega$B97X | $\omega$B97 | B97-1 | B3LYP | BLYP |
|---|---|---|---|---|---|
| MSE | 0.76 | 1.28 | 1.67 | −4.45 | −0.21 |
| MAE | 3.60 | 4.25 | 4.95 | 6.09 | 10.65 |
| rms | 4.52 | 5.41 | 7.79 | 8.98 | 16.91 |
| Max(−) | −5.96 | −6.50 | −15.29 | −37.51 | −50.36 |
| Max(+) | 14.88 | 18.14 | 25.44 | 9.62 | 55.26 |

TABLE VIII. Comparison of errors of different functionals for the reaction energies (in kcal/mol) of the 30 chemical reactions in the NHTBH38/04 and HTBH38/04 database (Refs. 55 and 56).

| Reactions | $\Delta E_{ref}$ | $\omega$B97X | $\omega$B97 | B97-1 | B3LYP | BLYP |
|---|---|---|---|---|---|---|
| $H+N_2O \rightarrow OH+N_2$ | $-65.08$ | 3.72 | 3.82 | 8.48 | 3.63 | 11.95 |
| $H+FCH_3 \rightarrow HF+CH_3$ | $-26.64$ | 3.37 | 4.27 | 4.55 | $-0.21$ | 0.48 |
| $H+F_2 \rightarrow HF+F$ | $-103.91$ | 0.50 | 2.21 | 3.43 | 0.20 | 10.08 |
| $CH_3+FCl \rightarrow CH_3F+Cl$ | $-52.74$ | $-1.85$ | $-2.60$ | $-0.64$ | 0.10 | 3.89 |
| $F^-+CH_3Cl \rightarrow FCH_3+Cl^-$ | $-32.65$ | $-1.29$ | 0.78 | $-2.33$ | $-2.17$ | 0.26 |
| $F^- \cdots CH_3Cl \rightarrow FCH_3 \cdots Cl^-$ | $-26.73$ | $-0.23$ | 1.17 | 0.20 | 0.35 | 3.96 |
| $OH^-+CH_3F \rightarrow HOCH_3+F^-$ | $-20.11$ | $-1.22$ | $-1.80$ | $-0.19$ | 0.14 | 1.25 |
| $OH^- \cdots CH_3F \rightarrow HOCH_3 \cdots F^-$ | $-36.24$ | $-1.62$ | $-1.36$ | $-2.09$ | $-1.52$ | $-0.26$ |
| $H+N_2 \rightarrow HN_2$ | 3.97 | $-4.30$ | $-3.57$ | $-5.12$ | $-7.37$ | $-7.23$ |
| $H+CO \rightarrow HCO$ | $-19.51$ | $-2.66$ | $-1.91$ | $-2.80$ | $-5.68$ | $-5.78$ |
| $H+C_2H_4 \rightarrow CH_3CH_2$ | $-40.03$ | $-2.97$ | $-3.52$ | 0.12 | $-1.89$ | 1.21 |
| $CH_3+C_2H_4 \rightarrow CH_3CH_2CH_2$ | $-26.12$ | $-4.05$ | $-5.65$ | $-1.53$ | 2.69 | 5.97 |
| $HCN \rightarrow HNC$ | 15.05 | $-1.87$ | $-1.97$ | $-1.69$ | $-0.99$ | 0.03 |
| $H+HCl \rightarrow H_2+Cl$ | $-3.0$ | 3.09 | 3.18 | 3.62 | $-1.49$ | $-1.28$ |
| $OH+H_2 \rightarrow H+H_2O$ | $-16.1$ | $-0.84$ | $-1.02$ | $-1.62$ | 3.25 | 2.22 |
| $CH_3+H_2 \rightarrow H+CH_4$ | $-3.2$ | $-2.30$ | $-2.86$ | $-2.97$ | 2.41 | 2.70 |
| $OH+CH_4 \rightarrow CH_3+H_2O$ | $-12.9$ | 1.46 | 1.84 | 1.35 | 0.84 | $-0.48$ |
| $OH+NH_3 \rightarrow H_2O+NH_2$ | $-9.5$ | 0.15 | 0.23 | $-0.27$ | $-0.44$ | $-1.51$ |
| $HCl+CH_3 \rightarrow Cl+CH_4$ | $-6.2$ | 0.79 | 0.33 | 0.65 | 0.92 | 1.41 |
| $OH+C_2H_6 \rightarrow H_2O+C_2H_5$ | $-16.5$ | 0.54 | 1.04 | 0.08 | $-0.19$ | $-1.98$ |
| $F+H_2 \rightarrow HF+H$ | $-31.6$ | $-1.46$ | $-1.96$ | $-2.39$ | 1.81 | $-0.71$ |
| $O+CH_4 \rightarrow OH+CH_3$ | 5.6 | $-0.50$ | 0.03 | $-1.54$ | $-3.26$ | $-5.84$ |
| $H+PH_3 \rightarrow PH_2+H_2$ | $-20.1$ | 0.61 | 0.74 | 1.14 | $-3.66$ | $-4.03$ |
| $H+HO \rightarrow H_2+O$ | $-2.4$ | 2.80 | 2.82 | 4.51 | 0.85 | 3.14 |
| $H+H_2S \rightarrow H_2+HS$ | $-13.8$ | 2.17 | 2.32 | 2.58 | $-2.34$ | $-2.43$ |
| $O+HCl \rightarrow OH+Cl$ | $-0.6$ | 0.29 | 0.36 | $-0.89$ | $-2.34$ | $-4.43$ |
| $NH_2+CH_3 \rightarrow CH_4+NH$ | $-14.4$ | 1.49 | 1.28 | 2.04 | 3.44 | 4.65 |
| $NH_2+C_2H_5 \rightarrow C_2H_6+NH$ | $-10.8$ | 2.41 | 2.08 | 3.32 | 4.47 | 6.16 |
| $C_2H_6+NH_2 \rightarrow NH_3+C_2H_5$ | $-7.0$ | 0.39 | 0.81 | 0.36 | 0.26 | $-0.47$ |
| $NH_2+CH_4 \rightarrow CH_3+NH_3$ | $-3.3$ | 1.21 | 1.50 | 1.53 | 1.18 | 0.94 |
| MSE | | $-0.07$ | 0.09 | 0.40 | $-0.23$ | 0.80 |
| MAE | | 1.74 | 1.97 | 2.13 | 2.00 | 3.22 |
| rms | | 2.10 | 2.36 | 2.80 | 2.66 | 4.36 |
| Max($-$) | | $-4.30$ | $-5.65$ | $-5.12$ | $-7.37$ | $-7.23$ |
| Max($+$) | | 3.72 | 4.27 | 8.48 | 4.47 | 11.95 |

set is used for all cases with counterpoise corrections[63] to reduce BSSE. The extrafine grid, EML(99,590), is used for the first three sets and the fine grid, EML(75,302), is used for the last three sets. Note that the sign convention for the first three sets (positive for stable molecules) is different from that for the last three sets (negative for stable molecules). As can be seen in Table IX, $\omega$B97X and $\omega$B97 perform best overall. This is largely because of relatively poor performance of B97-1, B3LYP, and BLYP for stacked base pairs, where unbound results can be incorrectly obtained.

### D. Equilibrium geometries

Satisfactory predictions of molecular geometries by density functionals are necessary for practical use. Geometry optimizations for each functional are performed on the equilibrium experimental test set (EXTS),[70] which consists of 166 symmetry unique experimental bond lengths for small to medium size molecules. The 6-311++G($3df$,$3pd$) basis set with the extrafine grid, EML(99,590), is used. As shown in Table X, performance of all of the hybrid functionals in predicting optimized geometries is similar, and clearly better than that of the pure density functional, BLYP.

### E. Dissociation of symmetric radical cations

Common semilocal functionals are generally accurate for systems near equilibrium. However, due to considerable self-interaction errors in semilocal functionals, spurious fractional charge dissociation occurs.[9,10,42] This situation becomes amplified for symmetric charged radicals $X_2^+$, such as $H_2^+$,[71] $He_2^+$,[72] $Ne_2^+$,[73] and $Ar_2^+$.[74] For such systems, the predicted DFA binding energy curves display a spurious energy barrier at intermediate bond length $R$. The Perdew–Zunger self-interaction correction[75] (PZ SIC) is usually used for minimizing the self-interaction errors in density functionals. However, the PZ SIC does not provide accurate results for equilibrium properties of molecules. Besides, the PZ SIC energy is not invariant with respect to unitary transforms of occupied orbitals, which makes this scheme more expensive than the usual KS-DFT calculations.

TABLE IX. Binding energies (in kcal/mol) of several sets of noncovalent interactions. The first three sets are taken from Ref. 69 with monomer deformation energies taken into considerations. The last three sets are taken from Ref. 57 without considering monomer deformation energies. The counterpoise corrections are applied for all the cases.

| Complex | $\Delta E_{ref}$ | $\omega$B97X | $\omega$B97 | B97-1 | B3LYP | BLYP |
|---|---|---|---|---|---|---|
| Charge-transfer complexes | | | | | | |
| $C_2H_4\cdots F_2$ | 1.06 | 1.03 | 1.09 | 1.58 | 1.22 | 2.40 |
| $NH_3\cdots F_2$ | 1.81 | 1.93 | 1.98 | 2.76 | 2.58 | 4.61 |
| $C_2H_2\cdots ClF$ | 3.81 | 4.43 | 4.50 | 4.54 | 3.54 | 4.09 |
| $HCN\cdots ClF$ | 4.86 | 5.32 | 5.42 | 4.77 | 4.32 | 4.50 |
| $NH_3\cdots Cl_2$ | 4.88 | 5.18 | 4.89 | 5.95 | 5.24 | 6.21 |
| $H_2O\cdots ClF$ | 5.36 | 6.16 | 6.21 | 5.80 | 5.32 | 5.69 |
| $NH_3\cdots ClF$ | 10.62 | 11.10 | 10.49 | 13.16 | 12.40 | 14.18 |
| MSE | | 0.39 | 0.31 | 0.88 | 0.32 | 1.33 |
| MAE | | 0.40 | 0.35 | 0.91 | 0.56 | 1.43 |
| Dipole-dipole interaction complexes | | | | | | |
| $H_2S\cdots H_2S$ | 1.66 | 1.99 | 1.99 | 1.53 | 0.76 | 0.56 |
| $HCl\cdots HCl$ | 2.01 | 2.30 | 2.33 | 1.78 | 1.09 | 0.87 |
| $H_2S\cdots HCl$ | 3.35 | 3.90 | 3.93 | 3.56 | 2.70 | 2.58 |
| $CH_3Cl\cdots HCl$ | 3.55 | 3.82 | 3.97 | 2.93 | 1.94 | 1.60 |
| $HCN\cdots CH_3SH$ | 3.59 | 3.99 | 4.05 | 3.39 | 2.47 | 2.05 |
| $CH_3SH\cdots HCl$ | 4.16 | 5.28 | 5.38 | 4.76 | 3.57 | 3.38 |
| MSE | | 0.50 | 0.56 | −0.06 | −0.97 | −1.21 |
| MAE | | 0.50 | 0.56 | 0.33 | 0.97 | 1.21 |
| Weak interaction complexes | | | | | | |
| $He\cdots Ne$ | 0.04 | 0.01 | −0.05 | 0.08 | −0.03 | −0.08 |
| $He\cdots Ar$ | 0.06 | 0.05 | −0.03 | 0.09 | −0.08 | −0.14 |
| $Ne\cdots Ne$ | 0.08 | −0.02 | −0.07 | 0.09 | −0.04 | −0.10 |
| $Ne\cdots Ar$ | 0.13 | 0.05 | −0.04 | 0.13 | −0.08 | −0.17 |
| $CH_4\cdots Ne$ | 0.22 | 0.10 | 0.00 | 0.16 | −0.10 | −0.21 |
| $C_6H_6\cdots Ne$ | 0.47 | 0.30 | 0.32 | 0.18 | −0.34 | −0.61 |
| $CH_4\cdots CH_4$ | 0.51 | 0.64 | 0.55 | 0.17 | −0.52 | −0.85 |
| MSE | | −0.05 | −0.12 | −0.09 | −0.39 | −0.52 |
| MAE | | 0.09 | 0.13 | 0.11 | 0.39 | 0.52 |
| Hydrogen-bonded DNA base pairs | | | | | | |
| $G\cdots A$ HB | −11.30 | −12.29 | −12.44 | −10.48 | −9.06 | −7.86 |
| $C\cdots G$ WC | −30.70 | −31.92 | −32.12 | −28.87 | −27.65 | −25.02 |
| $G\cdots C$ WC | −31.40 | −31.85 | −32.07 | −28.78 | −27.57 | −24.91 |
| MSE | | −0.89 | −1.08 | 1.76 | 3.04 | 5.20 |
| MAE | | 0.89 | 1.08 | 1.76 | 3.04 | 5.20 |
| Interstrand base pairs | | | | | | |
| $G\cdots G$ IS | −5.20 | −4.83 | −4.70 | −4.28 | −3.56 | −3.08 |
| $G\cdots G$ IS | 0.80 | 2.21 | 2.13 | 3.49 | 5.10 | 5.66 |
| $C\cdots C$ IS | 3.10 | 3.62 | 3.69 | 3.43 | 3.58 | 3.43 |
| MSE | | 0.77 | 0.80 | 1.31 | 2.14 | 2.44 |
| MAE | | 0.77 | 0.80 | 1.31 | 2.14 | 2.44 |
| Stacked base pairs | | | | | | |
| $A\cdots G$ S | −6.50 | −3.46 | −4.62 | 1.32 | 4.37 | 6.23 |
| $C\cdots G$ S | −12.40 | −8.57 | −9.61 | −4.14 | −1.33 | 0.44 |
| $G\cdots C$ S | −11.60 | −8.77 | −9.69 | −4.57 | −1.86 | −0.09 |
| MSE | | 3.23 | 2.19 | 7.70 | 10.56 | 12.36 |
| MAE | | 3.23 | 2.19 | 7.70 | 10.56 | 12.36 |
| MSE | | 0.51 | 0.36 | 1.29 | 1.41 | 2.01 |
| MAE | | 0.73 | 0.65 | 1.43 | 2.06 | 2.79 |

TABLE X. Statistical errors (in Å) of EXTS (Ref. 70).

| Error | $\omega$B97X | $\omega$B97 | B97-1 | B3LYP | BLYP |
|-------|-------|------|-------|-------|------|
| MSE | −0.003 | −0.002 | 0.004 | 0.003 | 0.018 |
| MAE | 0.009 | 0.010 | 0.008 | 0.008 | 0.019 |
| rms | 0.014 | 0.015 | 0.013 | 0.013 | 0.024 |
| Max(−) | −0.084 | −0.085 | −0.071 | −0.078 | −0.064 |
| Max(+) | 0.055 | 0.059 | 0.065 | 0.065 | 0.103 |

We perform unrestricted calculations with the aug-cc-pVQZ basis set and a high-quality EML(250,590) grid. The DFT results are compared with results from HF theory, and the very accurate CCSD(T) theory (coupled-cluster theory with iterative singles and doubles and perturbative treatment of triple substitutions).[76,77]

As shown in Table XI, the predicted bond length and binding energy of $\omega$B97X and $\omega$B97 are better than that of B97-1, B3LYP, and BLYP. Furthermore, the $\omega$B97X and $\omega$B97 functionals predict no spurious barriers on the dissociation curves and provide much improved results for $H_2^+$ and $Ar_2^+$ (see Fig. 1) relative to the common hybrid functionals. However, their results for $He_2^+$ (see Fig. 2) and $Ne_2^+$ are less satisfactory, as shown in Table XII.

To circumvent this, one needs to correct the remaining SIE by either using a larger $\omega$ (to approach full HF exchange faster) and/or by using a larger fraction of the $E_x^{SR-HF}$ (to reduce the remaining SR SIE). For both cases, a correlation functional more nonlocal than the $E_c^{B97}$ correlation is needed. Work along these lines is in progress.

### F. Long-range charge-transfer excitations

It has been shown by Dreuw et al. that pure DFA functionals qualitatively fail to describe long-range charge-transfer (CT) excitations between a donor and an acceptor.[11–13] Following Dreuw et al., we perform TDDFT calculations for the lowest CT excitations between ethylene and tetrafluoroethylene, when separated by a distance $R$.
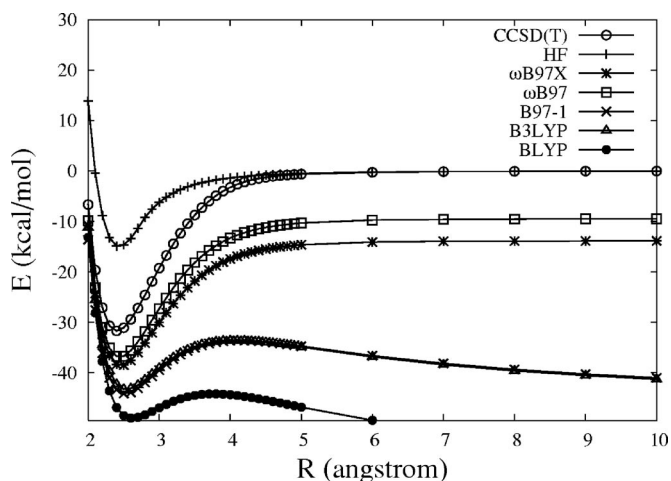


FIG. 1. Dissociation curve of $Ar_2^+$ curve. Zero level is set to E(Ar) +E(Ar$^+$) for each method.

During this process, an electron transfers from the highest occupied molecular orbital of tetrafluoroethylene to the lowest unoccupied molecular orbital of ethylene. The experimental geometry for each monomer $C_2H_4$ and $C_2F_4$ with the intermolecular distance $R=8$ Å was taken from Zhao and Truhlar.[78] Similarly, the geometries at different values of $R$ are obtained by varying the distance between their centers of mass without further reoptimzations. Calculations were performed using the 6-31G* basis set with the extrafine grid, EML(99,590). For comparison, high-level SAC-CI results are taken from Tawada et al.[38]

The correct CT excitation energy $\omega_{CT}(R)$ has the following asymptote:[11]

$$\omega_{CT}(R \rightarrow \infty) \approx -\frac{1}{R} + IP_{C_2F_4} - EA_{C_2H_4}, \tag{33}$$

where $IP_{C_2F_4}$ and $EA_{C_2H_4}$ are the ionization potential of tetrafluoroethylene and the electron affinity of ethylene, respectively.

TABLE XI. Dissociation energies of symmetric radical cations, $D_e = E(X) + E(X^+) − E(X_2^+, R_e)$ (in kcal/mol), where $R_e$ (in Å) is the equilibrium bond length. The reference values are taken from Ref. 71 for $H_2^+$, from Ref. 72 for $He_2^+$, from Ref. 73 for $Ne_2^+$, and from Ref. 74 for $Ar_2^+$.

| Molecule | Ref. | $\omega$B97X | $\omega$B97 | B97-1 | B3LYP | BLYP |
|----------|------|-------|------|-------|-------|------|
| | | | $R_e$ | | | |
| $H_2^+$ | 1.057 | 1.102 | 1.100 | 1.107 | 1.114 | 1.136 |
| $He_2^+$ | 1.081 | 1.137 | 1.141 | 1.146 | 1.146 | 1.184 |
| $Ne_2^+$ | 1.765 | 1.784 | 1.780 | 1.831 | 1.827 | 1.924 |
| $Ar_2^+$ | 2.423 | 2.457 | 2.445 | 2.519 | 2.536 | 2.621 |
| MSE | | 0.039 | 0.035 | 0.069 | 0.074 | 0.134 |
| MAE | | 0.039 | 0.035 | 0.069 | 0.074 | 0.134 |
| | | | $D_e$ | | | |
| $H_2^+$ | 64.4 | 68.4 | 68.5 | 68.9 | 67.9 | 69.1 |
| $He_2^+$ | 57.0 | 71.5 | 71.9 | 71.5 | 77.4 | 83.2 |
| $Ne_2^+$ | 32.2 | 54.0 | 56.0 | 58.5 | 59.4 | 73.1 |
| $Ar_2^+$ | 30.8 | 38.6 | 36.9 | 44.1 | 43.3 | 49.0 |
| MSE | | 12.0 | 12.2 | 14.7 | 15.9 | 22.5 |
| MAE | | 12.0 | 12.2 | 14.7 | 15.9 | 22.5 |
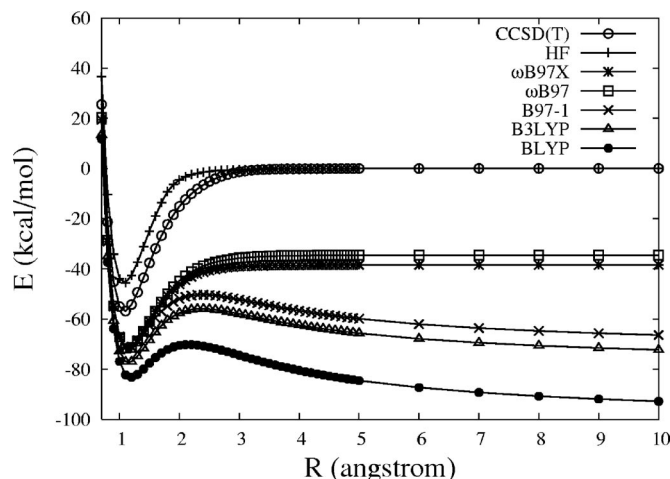
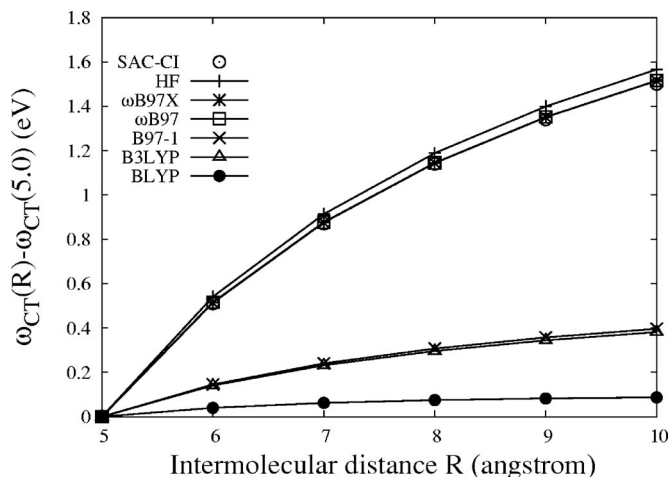FIG. 2. Dissociation curve of $He_2^+$ curve. Zero level is set to E(He) +E(He$^+$) for each method.



FIG. 3. The lowest CT excitation energy of $C_2H_4 \cdots C_2F_4$ dimer along the intermolecular distances $R$ (in Å). For all methods, the excitation energy at 5 Å is set to zero for each method.

As shown in Fig. 3, $\omega$B97X and $\omega$B97 predict CT excitation curves that are in an excellent agreement with the high-level SAC-CI results, while B97-1, B3LYP, and BLYP predict qualitatively incorrect CT excitation curves. This emphasizes the important role of the LC hybrid functionals in TDDFT, especially for CT excited states. However, both $\omega$B97X and $\omega$B97 are correct at long range by construction, but still have some short-range SIE. This can be seen in Fig. 4 where the same data are replotted showing the asymptotes for the charge-transfer state relative to the separated ground-state fragments. It is evident that errors are greatly reduced using $\omega$B97X and $\omega$B97 relative to functionals that are not long-range corrected, but there is still roughly 2 eV of remaining error. We are investigating the performance of these two new LC functionals on other types of excitation energies, such as valence excitations and Rydberg excitations.

## VI. CONCLUSIONS

We have developed two hybrid density functional models that include 100% long-range exact exchange, applying generalized gradient expressions for short-range exchange, and correlation that are of the form first suggested by Becke in his B97 functional.[20] This eliminates long-range self-interaction in the exchange functional, which is recognized to be physically important. Long-range and short-range exchanges are partitioned by the error function, Eq. (3), such that the short-range (SR) interaction approaches the full Coulomb interaction for $\omega=0$. The first functional, called $\omega$B97, includes no exact short-range exchange, while the second functional, called $\omega$B97X, includes a small fraction (about

16%) of exact short-range exchange. In this way, when the constraint of $\omega=0$ is applied, $\omega$B97X and $\omega$B97 reduce to the existing B97 and HCTH functional forms. Therefore these new functionals allow us to systematically explore the role of long-range exchange in improving the performance of these existing functionals.

The parameters in $\omega$B97X and $\omega$B97 were optimized on a diverse training set consisting of 412 data points, including atomization energies, barrier heights, intermolecular interaction energies, and atomic energies. The constraint of satisfying the uniform electron gas limit was enforced. The existing B97 (Ref. 20) and HCTH (Ref. 22) functional forms were also reoptimized on the same data set to enable direct comparison of the effect of long-range exchange. These constrained forms were both shown to provide significantly poorer quality of fits to the training data, indicating that the single extra degree of freedom corresponding to long-range exchange is physically important. Relaxing this constraint not only provides improved accuracy for the diverse systems in our training set, but also gives the exact long-range exchange potential that remedies some qualitative failures of hybrid functionals.
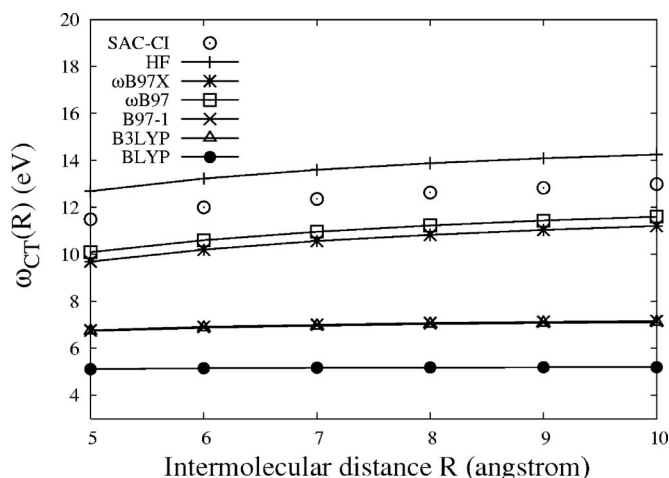
TABLE XII. Binding energies of symmetric radical cations at bond length $R=100$ (Å), $E_b=E(X_2^+, R=100$ (Å)$)-E(X)-E(X^+)$ (in kcal/mol).

| Molecule | $\omega$B97X | $\omega$B97 |
|---|---|---|
| $H_2^+$ | −21.3 | −17.9 |
| $He_2^+$ | −38.4 | −34.5 |
| $Ne_2^+$ | −34.7 | −33.6 |
| $Ar_2^+$ | −13.8 | −9.5 |



FIG. 4. The lowest CT excitation energy of $C_2H_4 \cdots C_2F_4$ dimer along the intermolecular distances $R$ (in Å).

Since $\omega$B97X and $\omega$B97 are parametrized functionals, we also test them against three well-established existing functionals [B97-1,[22] B3LYP,[14,16] and BLYP (Refs. [17] and [18])] on a separate independent test set of data, which includes further atomization energies, reaction energies, noncovalent interaction energies, equilibrium geometries, homonuclear diatomic cation dissociations, and a charge-transfer excited state. The results indicate that the new long-range corrected functionals are generally superior in performance for demanding cases such as atomization energies and base-stacking interactions. They are dramatically superior for dissociation and charge-transfer problems that are sensitive to self-interaction errors. This combination of better performance for standard calculations and greatly reduced errors for problems involving self-interaction means that $\omega$B97X and $\omega$B97 can be recommended for general use in chemistry, subject to some caveats which we discuss next.

As with all approximate density functionals, some limitations remain. While $\omega$B97X and $\omega$B97 are free of long-range self-interaction, they still suffer from some self-interaction at short range, which means that their performance for the demanding problems of homonuclear cation dissociation and charge-transfer excitations still shows significant errors relative to truly self-interaction free methods. Similarly, because the fraction of exact exchange is increased relative to "pure" functionals, in particular, their performance for systems with small gaps and thus potentially strong "static" correlation effects is not likely to be better than existing functionals. Finally, long-range correlation effects are not correctly treated in $\omega$B97X and $\omega$B97 (London forces are missing), and therefore systems and properties which are sensitive to this effect may not be accurately described. We hope to lift some of these limitations in future work.

## ACKNOWLEDGMENTS

[1] P. Hohenberg and W. Kohn, Phys. Rev. **136**, B864 (1964).
[2] W. Kohn and L. J. Sham, Phys. Rev. **140**, A1133 (1965).
[3] L. J. Sham and W. Kohn, Phys. Rev. **145**, 561 (1966).
[4] R. G. Parr and W. Yang, *Density-Functional Theory of Atoms and Molecules* (Oxford University Press, Oxford, 1989).
[5] R. M. Dreizler and E. K. U. Gross, *Density Functional Theory: An Approach to the Quantum Many Body Problem* (Springer-Verlag, Berlin, 1990).
[6] M. E. Casida, *Recent Advances in Density Functional Methods* (World Scientific, Singapore, 1995), Pt. 1.
[7] E. K. U. Gross, J. F. Dobson, and M. Petersilka, in *Density Functional Theory II* (Springer, Heidelberg, 1996).
[8] W. Kohn, A. D. Becke, and R. G. Parr, J. Phys. Chem. **100**, 12974 (1996).
[9] T. Bally and G. N. Sastry, J. Phys. Chem. A **101**, 7923 (1997); B. Braïda, P. C. Hiberty, and A. Savin, *ibid.* **102**, 7872 (1998); M. Grüning, O. V. Gritsenko, S. J. A. van Gisbergen, and E. J. Baerends, *ibid.* **105**, 9211

(2001); D. J. Tozer, N. C. Handy, and A. J. Cohen, Chem. Phys. Lett. **382**, 203 (2003); M. Lundberg and P. E. M. Siegbahn, J. Chem. Phys. **122**, 224103 (2005); P. Mori-Sánchez, A. J. Cohen, and W. Yang, *ibid.* **125**, 201102 (2006); A. Ruzsinszky, J. P. Perdew, G. I. Csonka, O. A. Vydrov, and G. E. Scuseria, *ibid.* **126**, 104102 (2007).
[10] A. D. Dutoi and M. Head-Gordon, Chem. Phys. Lett. **422**, 230 (2006).
[11] A. Dreuw, J. L. Weisman, and M. Head-Gordon, J. Phys. Chem. **119**, 2943 (2003).
[12] A. Dreuw and M. Head-Gordon, J. Am. Chem. Soc. **126**, 4007 (2004).
[13] A. Dreuw and M. Head-Gordon, Chem. Rev. (Washington, D.C.) **105**, 4009 (2005).
[14] A. D. Becke, J. Chem. Phys. **98**, 5648 (1993).
[15] A. D. Boese and J. M. L. Martin, J. Chem. Phys. **121**, 3405 (2004).
[16] P. J. Stephens, F. J. Devlin, C. F. Chabalowski, and M. J. Frisch, J. Phys. Chem. **98**, 11623 (1994).
[17] A. D. Becke, Phys. Rev. A **38**, 3098 (1988).
[18] C. Lee, W. Yang, and R. G. Parr, Phys. Rev. B **37**, 785 (1988).
[19] C. Møller and M. S. Plesset, Phys. Rev. **46**, 618 (1934).
[20] A. D. Becke, J. Chem. Phys. **107**, 8554 (1997).
[21] T. Van Voorhis and G. E. Scuseria, J. Chem. Phys. **109**, 400 (1998).
[22] F. A. Hamprecht, A. J. Cohen, D. J. Tozer, and N. C. Handy, J. Chem. Phys. **109**, 6264 (1998).
[23] P. J. Wilson, T. J. Bradley, and D. J. Tozer, J. Chem. Phys. **115**, 9233 (2001).
[24] T. W. Keal and D. J. Tozer, J. Chem. Phys. **123**, 121103 (2005).
[25] A. D. Boese, N. Doltsinis, N. C. Handy, and M. Sprik, J. Chem. Phys. **112**, 1670 (2000).
[26] A. D. Boese and N. C. Handy, J. Chem. Phys. **114**, 5497 (2001).
[27] Y. Zhao, N. E. Schultz, and D. G. Truhlar, J. Chem. Theory Comput. **2**, 364 (2006).
[28] A. D. Becke, J. Chem. Phys. **119**, 2972 (2003); **122**, 064101 (2005).
[29] J. D. Talman and W. F. Shadwick, Phys. Rev. A **14**, 36 (1976); V. Sahni, J. Gruenebaum, and J. P. Perdew, Phys. Rev. B **26**, 4371 (1982); T. Grabo, T. Kreibich, and E. K. U. Gross, Mol. Eng. **7**, 27 (1997).
[30] H. Stoll and A. Savin, in *Density Functional Methods in Physics*, edited by R. M. Dreizler and J. d. Providencia (Plenum, New York, 1985), p. 177.
[31] A. Savin, in *Recent Developments and Applications of Modern Density Functional Theory*, edited by J. M. Seminario (Elsevier, Amsterdam, 1996), pp. 327–357.
[32] T. Leininger, H. Stoll, H.-J. Werner, and A. Savin, Chem. Phys. Lett. **275**, 151 (1997).
[33] J. Toulouse, F. Colonna, and A. Savin, J. Chem. Phys. **122**, 014110 (2005).
[34] J. G. Ángyán, I. C. Gerber, A. Savin, and J. Toulouse, Phys. Rev. A **72**, 012510 (2005).
[35] E. Goll, H.-J. Werner, and H. Stoll, Phys. Chem. Chem. Phys. **7**, 3917 (2005).
[36] E. Goll, H.-J. Werner, H. Stoll, T. Leininger, P. Gori-Giorgi, and A. Savin, Chem. Phys. **329**, 276 (2006).
[37] H. Iikura, T. Tsuneda, T. Yanai, and K. Hirao, J. Chem. Phys. **115**, 3540 (2001).
[38] Y. Tawada, T. Tsuneda, S. Yanagisawa, T. Yanai, and K. Hirao, J. Chem. Phys. **120**, 8425 (2004).
[39] I. C. Gerber and J. G. Ángyán, Chem. Phys. Lett. **415**, 100 (2005).
[40] I. C. Gerber, J. G. Ángyán, M. Marsman, and G. Kresse, J. Chem. Phys. **127**, 054101 (2007).
[41] O. A. Vydrov, J. Heyd, A. V. Krukau, and G. E. Scuseria, J. Chem. Phys. **125**, 074106 (2006).
[42] O. A. Vydrov and G. E. Scuseria, J. Chem. Phys. **125**, 234109 (2006).
[43] J.-W. Song, T. Hirosawa, T. Tsuneda, and K. Hirao, J. Chem. Phys. **126**, 154105 (2007).
[44] A. J. Cohen, P. Mori-Sánchez, and W. Yang, J. Chem. Phys. **126**, 191109 (2007).
[45] P. M. W. Gill, R. D. Adamson, and J. A. Pople, Mol. Phys. **88**, 1005 (1996).
[46] R. D. Adamson, J. P. Dombroski, and P. M. W. Gill, J. Comput. Chem. **20**, 921 (1999).
[47] T. Yanai, D. P. Tew, and N. C. Handy, Chem. Phys. Lett. **393**, 51 (2004).
[48] J. P. Perdew and Y. Wang, Phys. Rev. B **45**, 13244 (1992).
[49] H. Stoll, C. M. E. Pavlidou, and H. Preuss, Theor. Chim. Acta **49**, 143 (1978); H. Stoll, E. Golka, and H. Preuss, *ibid.* **55**, 29 (1980).
[50] S. J. Chakravorty, S. R. Gwaltney, E. R. Davidson, F. A. Parpia, and C. F. Fischer, Phys. Rev. A **47**, 3649 (1993).

[51] L. A. Curtiss, K. Raghavachari, P. C. Redfern, and J. A. Pople, J. Chem. Phys. **106**, 1063 (1997).
[52] L. A. Curtiss, P. C. Redfern, K. Raghavachari, and J. A. Pople, J. Chem. Phys. **109**, 42 (1998).
[53] L. A. Curtiss, K. Raghavachari, P. C. Redfern, and J. A. Pople, J. Chem. Phys. **112**, 7374 (2000).
[54] J. A. Pople, M. Head-Gordon, D. J. Fox, K. Raghavachari, and L. A. Curtiss, J. Chem. Phys. **90**, 5622 (1989).
[55] Y. Zhao, B. J. Lynch, and D. G. Truhlar, J. Phys. Chem. A **108**, 2715 (2004).
[56] Y. Zhao, N. González-García, and D. G. Truhlar, J. Phys. Chem. A **109**, 2012 (2005); **110**, 4942(E) (2006).
[57] P. Jurečka, J. Šponer, J. Černý, and P. Hobza, Phys. Chem. Chem. Phys. **8**, 1985 (2006).
[58] E. Fromager, J. Toulouse, and H. J. A. Jensen, J. Chem. Phys. **126**, 074111 (2007).
[59] Y. Shao, L. Fusti-Molnar, Y. Jung, J. Kussmann, C. Ochsenfeld, S. T. Brown, A. T. B. Gilbert, L. V. Slipchenko, S. V. Levchenko, D. P. O'Neill, R. A. Distasio, Jr., R. C. Lochan, T. Wang, G. J. O. Beran, N. A. Besley, J. M. Herbert, C. Y. Lin, T. Van Voorhis, S. H. Chien, A. Sodt, R. P. Steele, V. A. Rassolov, P. E. Maslen, P. P. Korambath, R. D. Adamson, B. Austin, J. Baker, E. F. C. Byrd, H. Dachsel, R. J. Doerksen, A. Dreuw, B. D. Dunietz, A. D. Dutoi, T. R. Furlani, S. R. Gwaltney, A. Heyden, S. Hirata, C.-P. Hsu, G. Kedziora, R. Z. Khalliulin, P. Klunzinger, A. M. Lee, M. S. Lee, W. Liang, I. Lotan, N. Nair, B. Peters, E. I. Proynov, P. A. Pieniazek, Y. M. Rhee, J. Ritchie, E. Rosta, C. D. Sherrill, A. C. Simmonett, J. E. Subotnik, H. L. Woodcock, III, W. Zhang, A. T. Bell, A. K. Chakraborty, D. M. Chipman, F. J. Keil, A. Warshel, W. J. Hehre, H. F. Schaefer, III, J. Kong, A. I. Krylov, P. M. W. Gill, and M. Head-Gordon, Phys. Chem. Chem. Phys. **8**, 3172 (2006).
[60] P. M. W. Gill, B. G. Johnson, and J. A. Pople, Chem. Phys. Lett. **209**, 506 (1993).
[61] L. A. Curtiss, P. C. Redfern, K. Raghavachari, and J. A. Pople, J. Chem. Phys. **114**, 108 (2001).
[62] P. Mori-Sánchez, A. J. Cohen, and W. Yang, J. Chem. Phys. **124**, 091102 (2006).
[63] S. F. Boys and F. Bernardi, Mol. Phys. **19**, 553 (1970).
[64] L. A. Curtiss, P. C. Redfern, and K. Raghavachari, J. Chem. Phys. **123**, 124107 (2005).
[65] L. A. Curtiss, P. C. Redfern, and K. Raghavachari, J. Chem. Phys. **126**, 084108 (2007).
[66] Experimental values for Br atoms are taken from NIST-JANAF Thermochemical Tables, edited by M. W. Chase, Jr., fourth edition (1998). The enthalpy of formation at 0 K for gaseous Br atom $\Delta H_f^0$ (0 K) $=28.18$ kcal/mol, and the temperature correction $(H^{298}-H^0)$ $=2.929$ kcal/mol.
[67] C. W. Murray, N. C. Handy, and G. J. Laming, Mol. Phys. **78**, 997 (1993).
[68] V. I. Lebedev and D. N. Laikov, Dokl. Math. **59**, 477 (1999), and references therein.
[69] Y. Zhao and D. G. Truhlar, J. Phys. Chem. A **109**, 5656 (2005).
[70] R. A. DiStasio, Jr., R. P. Steele, Y. M. Rhee, Y. Shao, and M. Head-Gordon, J. Comput. Chem. **28**, 839 (2007).
[71] L. J. Schaad and W. V. Hicks, J. Chem. Phys. **53**, 851 (1970).
[72] J. Xie, B. Poirier, and G. I. Gellene, J. Chem. Phys. **122**, 184310 (2005).
[73] A. Carrington, D. I. Gammie, J. C. Page, A. M. Shaw, and J. M. Hutson, J. Chem. Phys. **116**, 3662 (2002).
[74] A. Wüest and F. Merkt, J. Chem. Phys. **120**, 638 (2004).
[75] J. P. Perdew and A. Zunger, Phys. Rev. B **23**, 5048 (1981).
[76] G. D. Purvis and R. J. Bartlett, J. Chem. Phys. **76**, 1910 (1982).
[77] K. Raghavachari, G. W. Trucks, J. A. Pople, and M. Head-Gordon, Chem. Phys. Lett. **157**, 479 (1989).
[78] Y. Zhao and D. G. Truhlar, J. Phys. Chem. A **110**, 13126 (2006).